Periodic traveling waves in nonlinear chains

Manuel Rodríguez-Achach* and Gabriel Pérez[†]
Departamento de Física Aplicada, CINVESTAV del IPN, Unidad Mérida
Apartado postal 73 "Cordemex", 97310 Mérida, Yucatán, México
Recibido el 10 de enero de 1996; aceptado el 17 de abril de 1996

ABSTRACT. The behavior of periodic traveling-wave solutions for three different nonlinear chains is studied. In all cases it is found that nontrivial solutions exist only for the sector of the frequency-wavenumber plane given by $\omega(k) \geq \omega_{\text{harmonic}}(k)$. There is a "dispersion relation" (understood here only as a functional relationship between frequency and wavenumbers) for each value of the average energy of the wave. In the case of the Fermi-Pasta-Ulam chain this result can be related, through scaling, with the existence of only one energy-independent dispersion curve for the harmonic chain. The limits of small amplitude and large wavelength are also explored, and used to implement different approximations to the traveling wave solution.

RESUMEN. En este artículo estudiamos el comportamiento de las soluciones de ondas viajeras periódicas para tres tipos de cadenas no lineales. En todos los casos encontramos que existen soluciones no triviales únicamente para un sector del plano frecuencia-número de onda, dado por $\omega(k) \geq \omega_{\text{armónica}}(k)$. Existe una "relación de dispersión" (que se debe entender sólo como una relación funcional entre la frecuencia y el número de onda), para cada valor de la energía promedio de la onda. En el caso de la cadena con potencial de Fermi-Pasta-Ulam, este resultado se puede relacionar, por medio de un reescalamiento, con la existencia de una sola relación de dispersión independiente de la energía para la cadena armónica. También se estudiaron los límites de pequeña amplitud y número de onda muy grande, y se utilizaron para implementar diferentes aproximaciones a la solución de onda viajera.

1. INTRODUCTION

Vibrations in solids can be treated very successfully in terms of the linearly independent modes of harmonic lattices, as it can be seen on any standard text on solid state physics [1, 2]. This fact sometimes makes one forget that interatomic interactions are fundamentally nonlinear in nature, a problem that is sometimes addressed a posteriori, with the introduction of nonlinear corrections to harmonic Hamiltonians. In most situations, characterized by small displacements of the atoms around their equilibrium locations, this approach is quite valid and gives good agreement with experimental results [2].

However, there is a lot to be said about the actual evolution of systems when their full nonlinearity is taken into account from the beginning, because very often the most interesting phenomena associated to nonlinearity is not accessible from perturbation theory. To give a simpleminded example, for a physical pendulum with potential $V(\theta) =$

---

* Electronic address: achach@kin.cieamer.conacyt.mx.
[†] Electronic address: gperez@kin.cieamer.conacyt.mx.

$mgl(1 - \cos\theta)$, the rotating solutions one has for $E > 2mgl$ cannot be obtained for any finite Taylor expansion of the potential. For a more complex example, the "kink" solitonic solution for a two-minimum quadratic-quartic potential has a singularity for its quartic coupling going to zero [3].

Large part of the research efforts in vibrations on nonlinear lattices has been concerned with their approximation by continuous media, which is valid for wavelengths much larger than the lattice spacing. In this limit, there has been extensive study of solitons, isolated perturbations that travel through the medium completely unchanged (a more restrictive definition of solitons require that they survive collisions [3, 4]). These solitary perturbations are remarkable in that they represent a perfect —and robust— equilibrium between the dispersive effects of the medium, and nonlinear effects that tend to give higher speed to large amplitude displacements, creating as a result shock waves [5]. Solitons have been found as exact solutions for many nonlinear wave equations, and besides their undeniable theoretical interest, are now being considered for technological applications, for instance, as carriers for communications via nonlinear fiber optics [6]. On the other hand, there are also some exact results for completely delocalized solutions for the vibrations of non-linear media, as is the case of the so-called "cnoidal waves" for the Korteweg-de Vries equation [7, 8]. These periodic solutions have received much less attention, and even their stability properties are not completely established [9, 10].

Compared with the continuum, there is a scarcity of results about the vibrations of fully discrete nonlinear lattices. In fact, the only known exact traveling wave solutions are those for the Toda chain [11]. Recently, some solutions for breathing modes with compact support were found for quartic chains [12], and there is also some numerical work in wide localized excitations, known as envelope solitons [13], and in narrow breathers, known as intrinsically localized modes [14–16]. For extended excitations, besides those of the Toda chain, there is some work in vibrational modes with special symmetries, for instance zone boundary modes [15, 17], where $k = \pi$. In general, much is still unknown about vibrations in nonlinear discrete chains.

In this work we will study fully extended modes, in the form of periodic traveling waves, in three different nonlinear chains. In Sect. 2 we present, for completeness, a short review of the most important properties of the harmonic chain. In Sect. 3 we present a model of an anharmonic chain with quartic potential, which was first treated by E. Fermi, J. Pasta and S. Ulam [19] in 1955. In Sect. 4 we show how traveling-wave solutions can be obtained from this model and the algorithm used for that purpose. We also discuss here the numerical results and the small amplitude and continuous limits. The Morse and Lennard-Jones potentials are discussed in Sect. 5 in an analogous way as it is done for the quartic potential model. In Sect. 6 we present our conclusions and discuss some open questions.

2. REVIEW OF THE HARMONIC CHAIN

The simplest vibrational behavior for a discrete chain is given by the Hamiltonian

$$H = \sum_n \frac{p_n^2}{2m} + \sum_n \frac{\kappa}{2}(u_{n+1} - u_n)^2,$$

where $u_n(t)$ are the displacements around the equilibrium positions of the particles in the chain. Equilibrium positions for successive particles are separated by a distance a, which we will take to be 1, fixing in this way the distance scale. We will also assume an infinite number of particles, so that boundary conditions can be ignored.

From this Hamiltonian one gets the equations of motion

$$\dot{p}_n = -\frac{\partial H}{\partial u_n} = \kappa(u_{n+1} - u_n) - \kappa(u_n - u_{n-1}),$$

$$\dot{u}_n = \frac{\partial H}{\partial p_n} = \frac{p_n}{m},$$

which combine to give a system of second order coupled differential equations

$$\ddot{u}_n = \Omega^2(u_{n+1} - 2u_n + u_{n-1}), \tag{1}$$

with $\Omega^2 = \kappa/m$ and n running over all integers. It is convenient at this moment to scale out the frequency parameter Ω by changing $t \to t/\Omega$, which is equivalent to setting the time units so that $\Omega = 1$. Under this transformations, the energy of the chain becomes

$$E(\{u_n\}; m, \kappa) \to m\Omega^2 E(\{u_n\}).$$

Due to the linearity of the equations of motion (1), they can be solved as a combination of elementary modes, where a mode is a solution of the form

$$u_n(t) = \text{Re}\left[ce^{i(nk-\omega t)}\right],$$

with c, k, and ω constants. Upon replacing this solution in the differential equation one gets a relationship between k and ω

$$\omega^2 = 4\sin^2 k/2, \tag{2}$$

which is the well known dispersion relation for the harmonic chain, a curve in the frequency-wavenumber plane. One usually confines k to $-\pi < k \leq \pi$ (first Brillouin zone). The average energy per particle associated to this mode is

$$E = m\Omega^2 \left[\omega^2 \frac{c^*c}{2}\right],$$

so all modes allow for any given value of energy, and the only restriction in the mode is the one imposed by the dispersion relation. If, for some value of the wavelength, we plotted energy vs. frequency, we will just get a vertical line at the correct value of ω, as given by the dispersion relation (2). We may choose to interpret this fact as an example of degeneracy, where a physical state allows for any value for the energy, irrespective of other parameters.

3. QUARTIC POTENTIAL: THE FERMI-PASTA-ULAM CHAIN

In this section we review the so called FPU system, a model that was investigated numerically at the beginning of the computer age [19]. It was expected to observe the relaxation to equipartition of energy among the linear normal modes of the system, but the numerical simulation actually showed that the energy of the initially excited mode was shared only with the first few modes. Even more surprising was the fact that almost all of the energy flows back to the initial mode at longer times. Later investigations revealed that energy equipartition can be reached, but at sufficiently high energies, where a transition to chaotic behavior is observed in the system [17, 18].

The Hamiltonian for this model is

$$H_{\text{FPU}} = \sum_n \frac{p_n^2}{2m} + \sum_n \frac{\kappa}{2}(u_{n+1} - u_n)^2 + \sum_n \frac{\beta}{4}(u_{n+1} - u_n)^4,$$

where the potential term can stand on its own or be taken to be the first two terms of the expansion for some nonlinear potential without cubic terms. In order to have the Hamiltonian bounded from below, we require $\beta > 0$. However, κ is allowed to have any real value, which for $\kappa < 0$ gives us potentials with two minima, which in turn can give rise to symmetry breaking rest states and topological solitons, due to the existence of two different minima for the energy [3]. Here we will keep $\kappa > 0$ and concentrate only in extended solutions.

The equations of motion for the system are now

$$\ddot{u}_n = (\kappa/m)(u_{n+1} - u_n) - (\kappa/m)(u_n - u_{n-1})$$
$$+ (\beta/m)(u_{n+1} - u_n)^3 - (\beta/m)(u_n - u_{n-1})^3,$$

which because of their nonlinearity can no longer be solved as a superposition of elementary modes. The two parameters here can be scaled out with the replacements

$$u_n \rightarrow \sqrt{\kappa/\beta}\, u_n; \qquad t \rightarrow \sqrt{m/\kappa}\, t = t/\Omega,$$

so that time is measured now in units of $1/\Omega$ and the amplitude of the oscillations in units of $\sqrt{\kappa/\beta}$ (notice that this implies the use of different units for the interparticle distance and the amplitude of oscillations). The resulting equation of motion is the simpler one

$$\ddot{u}_n = u_{n+1} + u_{n-1} - 2u_n + (u_{n+1} - u_n)^3 - (u_n - u_{n-1})^3. \tag{3}$$

This scaling has very important consequences, since its application to the energy results in the transformation

$$E_{\text{FPU}}(\{u_n\}; m, \kappa, \beta) \rightarrow \frac{\kappa^2}{\beta} E_{\text{FPU}}(\{u_n\}), \tag{4}$$

from where we see that, if we have a traveling wave solution for the scaled Eqs. (3), and try to take $\beta \rightarrow 0$ (approach the limit of the harmonic chain), we get diverging energies.

4. Periodic traveling-wave solutions

Of all the possible solutions to the equations of motion (3) we will concentrate in a very reduced set. Let us consider only those solutions that obey

$$u_{n+1}(t) = u_n(t - 1/v),$$

where v is a constant velocity (remember that we took the distance between particles to be 1). This makes the solutions into traveling waves of the form $u_n(t) = u(t - n/v)$. Besides this, we will also require that the solutions be periodic:

$$u(t) = u(t + T).$$

These two conditions are very restrictive, and allow us to find unique solutions to Eqs. (3). These periodic traveling waves have also associated to them a frequency $\omega = 2\pi/T$ and a wavenumber $k = \omega/v$, allowing us to introduce the concept of energy-dependent "dispersion relations", understood here only as the functional relationship between frequency and wavenumber for some given value of energy. It should be clear that there is no relation between this and the actual dispersion of a wavepacket in a linear chain, since these traveling waves cannot be superposed.

Introducing the definition $t_0 \equiv 1/v$, the equations of motion now become

$$\ddot{u}(t) = u(t + t_0) + u(t - t_0) - 2u(t)$$
$$+ \left(u(t + t_0) - u(t)\right)^3 - \left(u(t) - u(t - t_0)\right)^3. \tag{5}$$

This is now a delayed-advanced ordinary differential equation, with an extra condition of periodicity. These equations are invariant with respect to the addition of a constant, $u(t) \rightarrow u(t) + C$. We will fix this constant by making the average value of $u(t)$ equal to zero. Since the potential is even in u, and Eq. (5) is invariant under an inversion in the time direction, we can use the symmetry conditions $u(t) = u(T/2 - t)$ and $u(-t) = -u(t)$. This last two conditions are quite general and do not restrict the problem more than the periodicity condition does.

4.1. Algorithm for numerical solution

The algorithm for the solution is based in a finite difference method [20] where the equation of motion (5), written as

$$\ddot{u}(t) = F\left(u(t + t_0), u(t - t_0), u(t)\right),$$

is discretized on a mesh with timestep $\Delta t \ll T$, such that $t \rightarrow j\Delta t$, with j integer, and where $t_0 \rightarrow j_0 \Delta t$ and $T \rightarrow M\Delta t$. The mesh is finite and contains M points. For convenience, we will denote from now on $u(t) = u(j\Delta t) \equiv u^j$. The second derivative can be approximated to order $(\Delta t)^2$ by

$$\ddot{u}(t) \rightarrow D^2(u^j) \equiv \frac{u^{j+1} + u^{j-1} - 2u^j}{(\Delta t)^2} + \mathcal{O}(\Delta t)^2,$$

or, to next order, by

$$\ddot{u}(t) \to D^2(u^j) \equiv \frac{-u^{j+2} + 16u^{j+1} - 30u^j + 16u^{j-1} - u^{j-2}}{12(\Delta t)^2} + \mathcal{O}(\Delta t)^4.$$

The force term is replaced by

$$F\left(u(t+t_0), u(t-t_0), u(t)\right) = F\left(u^{j+j_0}, u^{j-j_0}, u^j\right),$$

and we impose boundary conditions $u^0 = u^M = 0$, and periodicity by $u^{j+M} = u^j$. The two symmetries we have discussed allow us to solve only for $M/4$ points in the mesh. The equations to solve become now

$$G(u^j) = D^2(u^j) - F(u^{j+j_0}, u^{j-j_0}, u^j) = 0; \qquad j = 1, 2 \ldots M,$$

and the solution is achieved with a Newton-Raphson multivariable routine. The quality of the results is checked by increasing the number of points in the mesh, and by comparing the effect of using second or fourth order approximations in the derivative term. In all numerical work presented here, these checks show only negligible changes in the solutions.

4.2. Numerical results

We have found periodic traveling wave solutions for the FPU chain. Their most important characteristic is that they exist only for values of ω and k such that $\omega(k) > \omega_{\mathrm{h}}(k) \equiv 2\sin(k/2)$, and they are therefore "supersonic waves". The harmonic dispersion relation acts as a boundary in the k–ω plane between nontrivial solutions and zero solutions. When ω is close to, but above the harmonic value, the amplitude of the solutions is small and their shapes are almost sinusoidal (Fig. 1). As we raise ω away from ω_{h}, or approach $k = 0$ or $k = 2\pi$, for a given ω, the amplitude grows and the shape becomes closer to that of a rectangular step (Fig. 2). Notice that we choose to plot the amplitude of the wave vs. time. We could have chosen to use the lattice site coordinate n instead of the time; however, remember that the solutions are traveling waves which obey the relation $u_n(t) = u(t - n/v)$, so it makes no difference to use t or n, apart from the fact that using n as coordinate would produce a discrete graph.

We calculate the average energy per particle using

$$E = \frac{1}{T} \int_0^T dt \left[\frac{\dot{u}^2(t)}{2} + V(u(t), u(t+t_0), u(t-t_0)) \right], \tag{6}$$

and obtain energy vs. ω plots as the one shown in shown in Fig. 3, and energy vs. k plots as that of in Fig. 4. Notice that the energy curve for nontrivial solutions starts from ω_{h} with nonzero slope. In Fig. 5 we show the energy surface in the $k = \omega$ plane, which shows very clearly the absence of periodic traveling wave solutions for $\omega(k) < \omega_{\mathrm{h}}(k)$. For any given nonzero value of the energy, the corresponding transversal cut of this surface gives the "dispersion relation", i.e., the allowed functional relationship between ω and k. The
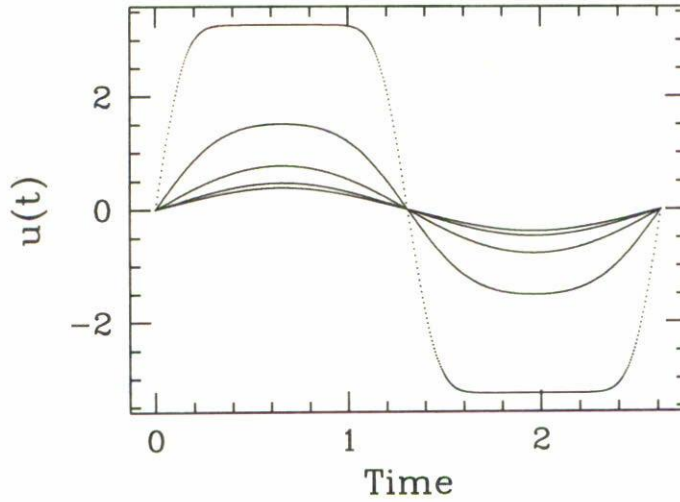
FIGURE 1. Waveforms for 4 different periodic traveling wave solutions for the FPU chain. Here we have fixed $\omega = 2.4$, and the values of k are, in increasing order of magnitude, $1.2 \times \pi$, $1.4 \times \pi$, $1.6 \times \pi$, and $1.8 \times \pi$. The differential equation (5) was discretized on a mesh of 480 points.
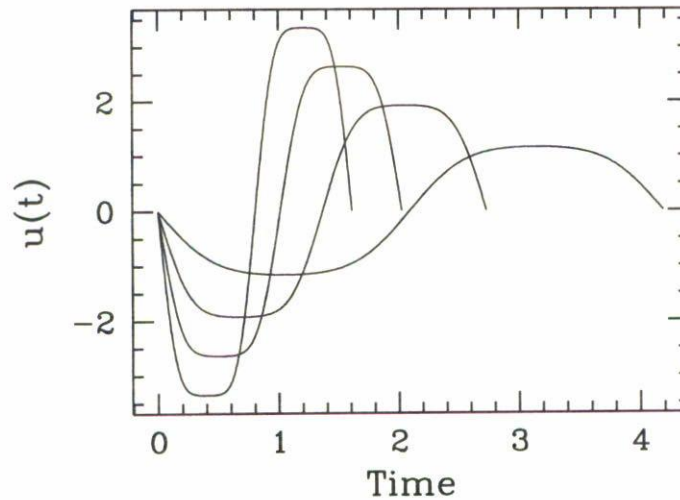

FIGURE 2. Waveforms for 4 different periodic traveling wave solutions for the FPU chain. Here we have fixed $k = 1.0$, and the values of ω are, in increasing order of magnitude, 1.5, 2.3, 3.1, and 3.9. The differential equation (5) was discretized on a mesh of 480 points.

harmonic dispersion curve corresponds to a cut taken at $E = 0^{+}$. These curves also seem to converge at $\omega = 0$ for $k \to 0$ and $k \to 2\pi$, meaning that energy diverges at these two values of k.

From this surface it is also quite clear how the scaling (4) of the Hamiltonian selects the harmonic curve as $\beta \to 0$. In this limit, zero energy remains zero (no solutions), and any solutions with finite energy see their energy diverge. So, as we make β close to zero, only a narrow band of states whose "dispersion relation" (their value of ω for a given k) is close to that given by the harmonic curve will retain moderate values for their energies,
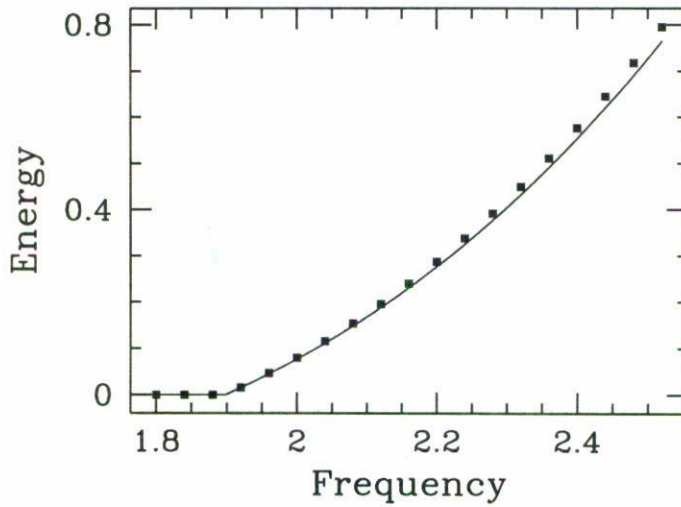
FIGURE 3. Energy per particle as a function of frequency for the FPU chain. Here $k = 2.5$. The squares correspond to the solutions obtained using finite differences, and the continuous line to the approximation given by the optimal amplitude sine wave, Eqs. (9) and (10).
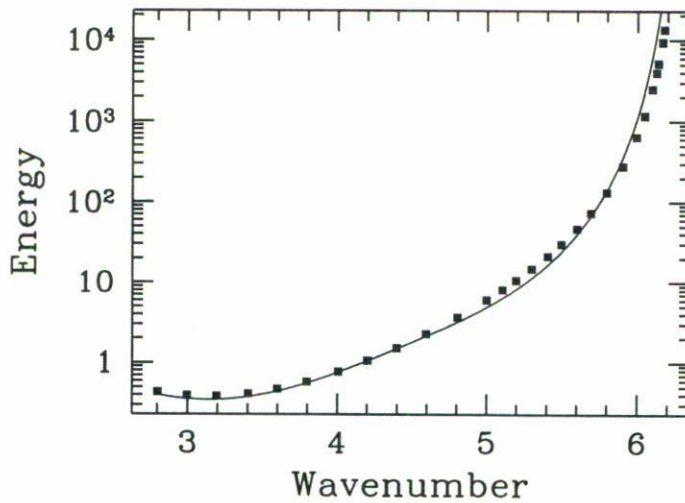

FIGURE 4. Energy per particle as a function of wavenumber for the FPU chain. Here $w = 2.4$. The squares correspond to the solutions obtained using finite differences, and the continuous line to the approximation given by the optimal amplitude sine wave, Eqs. (9) and (10). This energy diverges as k approaches 0 or 2π.

and for the limit $\beta = 0$, only the states sitting just above the harmonic curve, having energies infinitesimally close to zero, will have nonzero finite energies.

4.3. Small amplitude limit

From the numerical results shown in Figs. 1 and 2 it is apparent that the small amplitude oscillations of the chain fit almost perfectly a sinusoidal shape, as they should. This is to
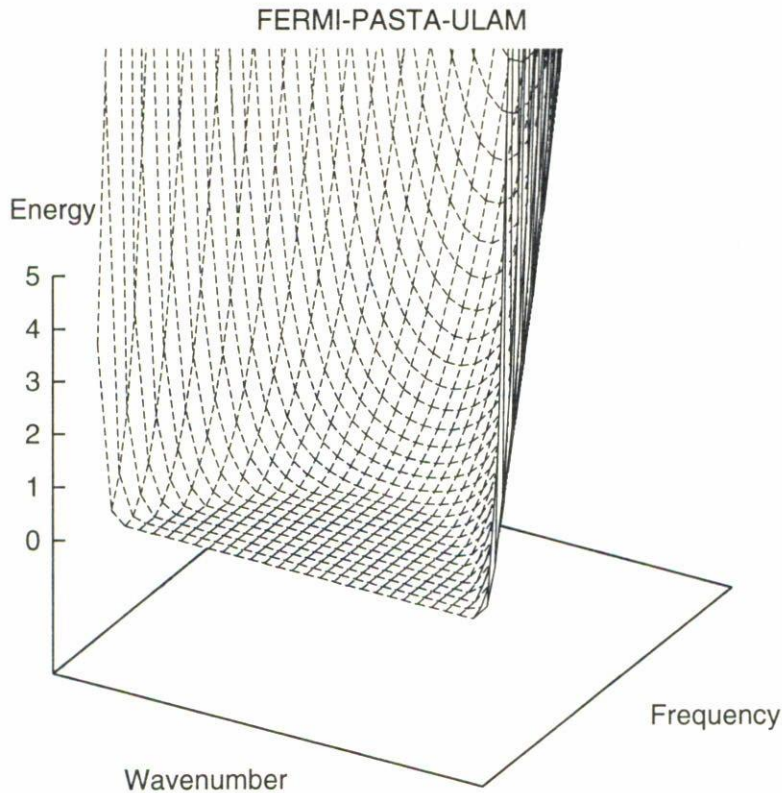
FIGURE 5. Energy surface for the FPU chain, as obtained from the finite differences method. The regions of k close to 0 and π are not given because the numerical algorithms start to fail in those sectors. The wavenumber goes from 0 to 2π and the frequency from 0 to 4.

be expected from the differential equation, and is just a numerical realization of the small oscillation approach that is customarily used as a first approximation to the dynamics of arbitrary potentials [21]. An interesting question to ask here is how close to the actual solution a simple sinusoidal wave can be. For this purpose we take the approximated solution $u(t) \approx A\sin(\omega t)$, and consider the normalized squared error in the differential equation, defined by

$$\text{Err} = \frac{\int_0^T dt\,[\ddot{u} - F(u(t), u(t+t_0), u(t-t_0))]^2}{\int_0^T dt\,u^2(t)}. \tag{7}$$

In practice, what we do here is to fit a lowest order Fourier expansion for the actual traveling wave. We use the normalized error instead of the total error given by the numerator in Eq. (7) in order to avoid the $A = 0$ trivial minimum. The error we obtain is a function of A^2, and can be written as

$$\text{Err} = C_4 A^4 + X C_2 A^2 + X^2,$$

where the different coefficients are defined by

$$X = \omega^2 - 4\sin^2(k/2) = \omega^2 - \omega_{\text{h}}^2,$$

$$C_2 = -\tfrac{3}{2}\omega_{\mathrm{h}}^4, \tag{8}$$

$$C_4 = \tfrac{1}{8}\omega_{\mathrm{h}}^8 \left(\tfrac{1}{2}\omega_{\mathrm{h}}^4 - 3\omega_{\mathrm{h}}^2 + 9 \right).$$

When we minimize this error with respect to A^2 we get

$$A^2 = \frac{12(\omega^2 - \omega_{\mathrm{h}}^2)}{\omega_{\mathrm{h}}^4(\omega_{\mathrm{h}}^4 - 6\,\omega_{\mathrm{h}}^2 + 18)}. \tag{9}$$

Therefore, one gets here that there is a real value for the amplitude A only if $\omega^2 \geq \omega_{\mathrm{h}}^2$ (note that the expression in the denominator is a positive definite quadratic form), and that amplitude goes to zero as $\omega \to \omega_{\mathrm{h}}$ from above. The energy associated to this minimum is

$$E(\omega, k) = \frac{A^2(\omega, k)}{4} \left(\omega^2 + \omega_{\mathrm{h}}^2 + \tfrac{3}{8}A^2(\omega, k)\omega_{\mathrm{h}}^4 \right). \tag{10}$$

This energy diverges as we take $k \to 0$ or $k \to 2\pi$, where $\omega_{\mathrm{h}} \to 0$, for all $\omega > \omega_{\mathrm{h}}$. This effect is also quite clear in the numerical work, where solutions start to grow out of numerical reach for values of k near these two limits. Even though the actual wavefunctions become very non-sinusoidal as we approach $k = 0$ or $k = \pi$, the approximated energy (10) gives a very good agreement with the actual energy of the chain, for the whole k range (see Fig. 4). Notice also that, for ω close to ω_{h}, $A^2 \approx \omega - \omega_{\mathrm{h}}$, and therefore $E \approx \omega - \omega_{\mathrm{h}}$, explaining the linear behavior found for E for small amplitudes.

4.4. Continuous limit

For traveling waves with wavelength much larger than the lattice spacing, a continuous approximation can be made. Assuming the change in the wavefunctions from site to site is small, we can take $u_n(t)$ into $u(t, x)$, where $x \equiv na$, and then use the approximations

$$u_{n\pm 1}(t) \equiv u(t, x \pm a) \approx u(t, x) \pm a\frac{\partial u(t, x)}{\partial x} + \frac{a^2}{2}\frac{\partial^2 u(t, x)}{\partial x^2} \pm \frac{a^3}{6}\frac{\partial^3 u(t, x)}{\partial x^3} + \cdots. \tag{11}$$

Here we are, for the moment being, writing explicitly the lattice constant as a. We will take $a = 1$ later on. Plugging this approximations in the equations of motion (3), keeping terms up to fourth order, we get a partial differential equation [22]

$$\frac{\partial^2 u}{\partial t^2} = a^2\frac{\partial^2 u}{\partial x^2} + \frac{a^4}{12}\frac{\partial^4 u}{\partial x^4} + 3a^4\frac{\partial^2 u}{\partial x^2}\left(\frac{\partial u}{\partial x}\right)^2,$$

plus terms of order $(a/\lambda)^6$. If we want to restrict ourselves to traveling waves $u(x, t) = u(x \pm vt)$, we obtain finally an ordinary differential equation (taking $a = 1$)

$$u'''' + 12\left[1 - v^2 + 3(u')^2\right]u'' = 0, \tag{12}$$

where the primes denote derivatives with respect to the argument $z \equiv x \pm vt$; if we integrate with respect to it we get

$$u''' + 12[1 - v^2 + (u')^2]u' + a = 0. \tag{13}$$

Multiplying by u'' and performing another integration we obtain,

$$(u'')^2 + 12(1 - v^2)(u')^2 + 6(u')^4 + 2au' - b^2 = 0.$$

For the integration of this equation we want to use the initial conditions $u(0) = u'(0) = u'''(0) = 0$, fixing an arbitrary initial value for $u''(0)$. From here we get $a = 0$ and $b = u''(0)$. This choice assumes that we start from a minimum of the function, which we can set to be zero because of the independence of the equations with respect to u, and that we are explicitly using the symmetries of the potential to set $u''' = 0$ at that point.

Putting $y = u'$, we arrive at the following equation:

$$t = \int_0^Y \frac{dy}{\sqrt{-6y^4 + 12(v^2 - 1)y^2 + b^2}},$$

which is an elliptic integral. The solutions can be expressed in terms of Jacobi elliptic functions [23], and correspond to the "cnoidal" solutions for the continuous limit of the FPU chain, usually expressed in terms of the modified Korteweg-de Vries equation [4, 10]. For our purposes here, it is more practical to perform a numerical integration of Eq. (13).

Results of the numerical integration of this differential equation are shown in Fig. 6. They are only qualitatively correct, probably because the approximations involved in going to a continuous description are too strong for the examples we are giving here. The integrated functions are periodic, have the expected symmetries, and their shapes correspond to the smoothed step forms of the actual solution, becoming more step-like as k is reduced. However, the amplitude of the solutions does not change much with changes in $u''(0)$, and therefore the traveling wave and its associated energy are quantitatively wrong. We have verified that this difficulty remains even as we adjust ω to values close to ω_h, where the amplitude of the wave is expected to go to zero.

5. Morse and Lennard-Jones potentials

In the modeling of real physical systems, one needs to have potentials that go to zero at infinity, since interparticle forces acting at macroscopic and atomic level always decay at long distances. In the other hand, one usually wants these potentials to grow, even to diverge, as the interparticle distance decreases. Two important and often used potentials with these characteristics are the Morse potential

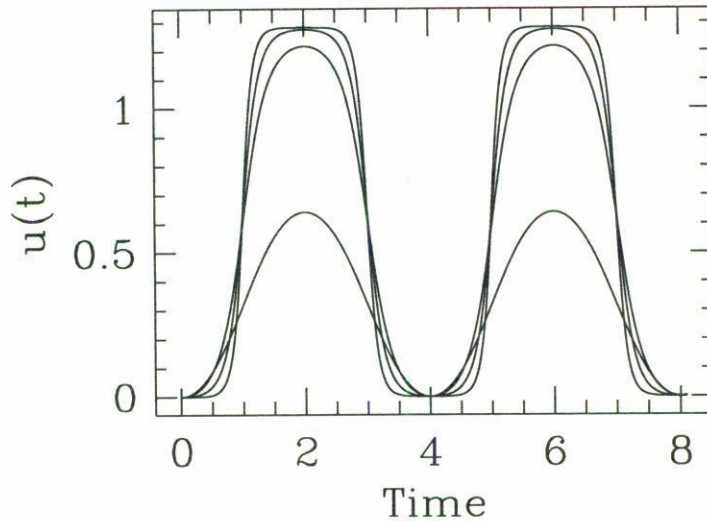$$V_M(R) = V_0 \left(1 - Ae^{-b(R-R_0)}\right)^2,$$

FIGURE 6. Waveforms for 4 different periodic traveling wave solutions for the FPU chain, obtained solving the differential equation (13).

and the Lennard-Jones (LJ) potential

$$V_{\mathrm{LJ}}(R) = V_0 \left[\left(\frac{R_0}{R} \right)^{12} - \left(\frac{R_0}{R} \right)^6 \right],$$

where R denotes the interparticle distance and R_0 is a distance scale parameter. Morse potentials are often used in molecular physics and chemistry for modeling interatomic interactions, while the LJ potential, which can be shown to originate with induced dipole-dipole interaction, is common in the simulation of liquids [24, 25]. This later potential diverges at $R = 0$, while Morse potential remains finite for all finite R.

In order to compare with the results obtained for the FPU system, we need first to scale the parameter in these two potentials so that their minima be located at $R = 1$ and the quadratic and quartic term of an expansion around this point agree with the two terms in the FPU model. For the Morse potential this means that we will require

$$R_0 = 1 - \frac{\ln(A)}{b} \implies V_{\mathrm{M}}(R) = V_0 \left(1 - e^{-b(R-1)} \right)^2.$$

Expanding up to fourth order in $R - 1$ we find

$$V_{\mathrm{M}}(R) \approx b^2 V_0 (R-1)^2 - b^3 V_0 (R-1)^3 + \tfrac{7}{6} b^4 V_0 (R-1)^4 + \dots$$

so that, comparing with the two terms for the scaled FPU potential, and taking $m = 1$ for convenience, one gets that $b = \sqrt{6/7}$ and $V_0 = 7/12$.

For the LJ potential, the requirement that the equilibrium distance be one makes $R_0 = (1/2)^{1/6}$, and the fixing the quadratic term in the expansion to be the same as that of the FPU potential means that V_0 should be 1/36. Since we introduced the LJ potential

with only two parameters, we do not get to fix the coefficient of the quartic term in the expansion. It should be noticed that, while a power-series expansion of the Morse potential around its minimum is convergent for all R, the LJ potential has zero convergence radius around its minimum, and therefore the expansions one makes in order to fix the coefficients are only formal. This fact does not seem to affect much the results for the numerical integrations.

Using now these normalized expressions as interparticle potentials for an infinite linear chain with rest lattice spacing equal to one, one gets the Hamiltonians

$$H_\mathrm{M} = \sum_n \frac{p_n^2}{2} + \sum_n \frac{7}{12}\left(1 - e^{-\sqrt{6/7}(u_{n+1}-u_n)}\right)^2,$$

and

$$H_\mathrm{LJ} = \sum_n \frac{p_n^2}{2} + \sum_n \frac{1}{36}\left[\frac{1}{2(u_{n+1}-u_n+1)^{12}} - \frac{1}{(u_{n+1}-u_n+1)^6}\right].$$

The work done for these two nonlinear chains reproduces the steps already taken for the FPU chain, except that the equations of motion are not symmetric under the interchange $u \to -u$, unless we reverse the n indexing of the chain. Therefore we no longer have the symmetry $u(t) = u(T/2 - t)$. This means that we need to solve now for half a period, instead of $T/4$ as we did in the case of FPU. Therefore, this limiting solutions have a half-wavelenght symmetry, in contrast to the FPU solutions which exhibit a quarter-wavelenght symmetry.

The behavior of the Morse and LJ systems for ω close to the harmonic value ω_h is, as expected, analogous to the FPU system, that is, we get small amplitude solutions that are almost sinusoidal. However, as we raise the ω value, the shape of the solutions becomes closer to that of a saw-tooth wave, as we see in Figs. 7 and 8. Note that this solutions are essentially the same, except for the greater amplitude in the Morse case. This reflects the fact that this potentials have the same qualitative behavior. Again, nontrivial solutions are only found for $\omega(k) > \omega_\mathrm{h}(k)$; this can be seen in Figs. 9 and 10, and in the energy surface plot in Fig. 11.

5.1. Small amplitude limit

Assuming as before a simple $u(t) = A\sin(\omega t)$ solution for the dynamics of either the LJ or the Morse chains, one can implement a numerical minimization of the normalized error given by Eq. (7), in order to find the best fitting sinusoidal approximation for periodic traveling waves. It was found however that for these potentials this procedure does not yield the correct behavior for A when $\omega \to \omega_\mathrm{h}$, except for $k = \pi$. To understand where the problem lies, one needs to expand any of these chain potentials up to fourth order terms in the form

$$V(\{u_n\}, C_3) \approx \sum_n \left[\frac{1}{2}(u_{n+1} - u_n)^2 + \frac{C_3}{3}(u_{n+1} - u_n)^3 + \frac{1}{4}(u_{n+1} - u_n)^4\right],$$
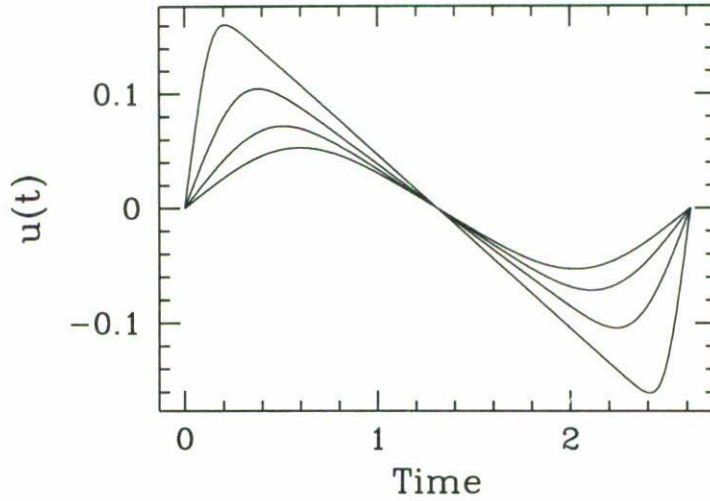
FIGURE 7. Waveforms for 4 different periodic traveling wave solutions for the LJ chain. Here we have fixed $\omega = 2.4$, and the values of k are, in increasing order of amplitude, $1.2 \times \pi$, $1.4 \times \pi$, $1.6 \times \pi$, and $1.8 \times \pi$. The corresponding differential equation was discretized on a mesh of 400 points.
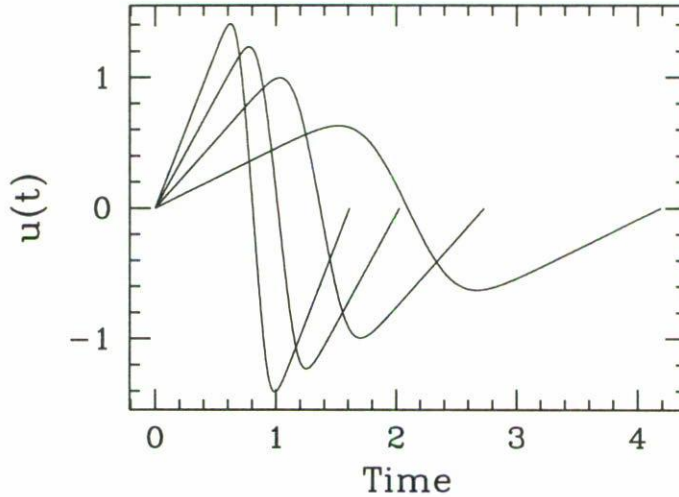

FIGURE 8. Waveforms for 4 different periodic traveling wave solutions for the Morse chain. Here we have fixed $k = 1.0$, and the values of ω are, in increasing order of amplitude, 1.5, 2.3, 3.1, and 3.9. The corresponding differential equation was discretized on a mesh of 400 points.

where we have as before scaled out the coefficients of the quadratic and quartic terms, and are left with only one parameter. For this expanded potential, the normalized error is given by

$$\text{Err} = C_4 A^4 + X C_2 A^2 + \tfrac{1}{4} W^2 A^2 + X^2,$$

where X, C_4 and C_2 are as given in Eq. (8), and W^2 is given by

$$W^2 = C_3^2 \omega_{\text{h}}^4 (4\omega_{\text{h}}^2 - \omega_{\text{h}}^4).$$
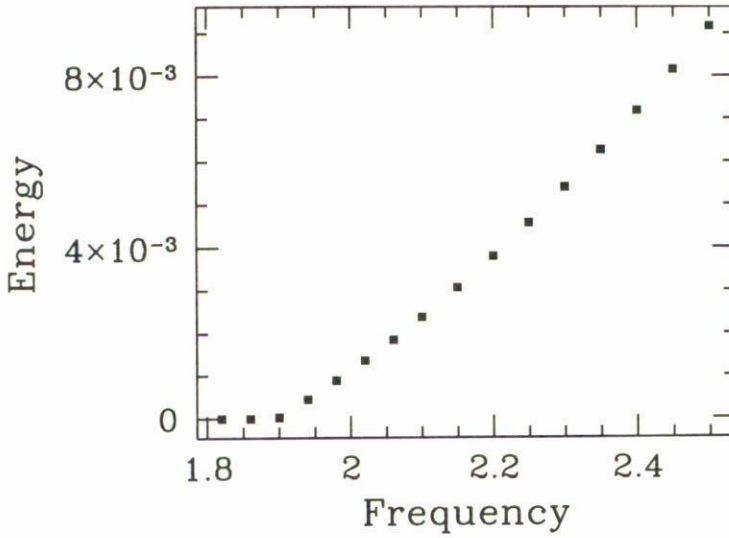
FIGURE 9. Energy per particle as a function of frequency for the LJ chain. Here $k = 2.5$. The solutions were obtained using the finite difference approach.
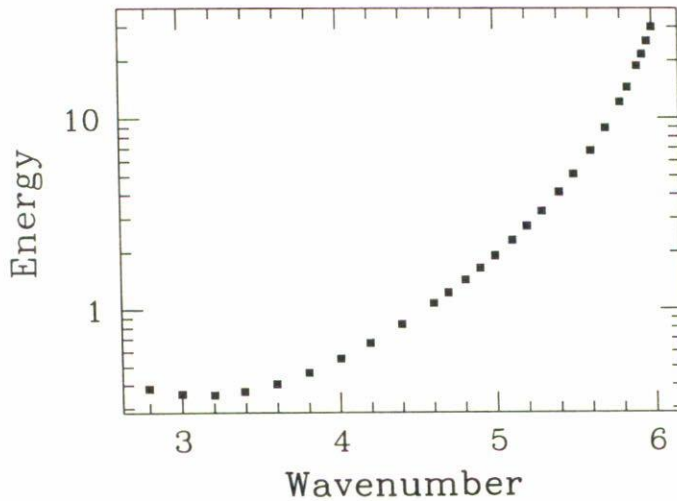

FIGURE 10. Energy per particle as a function of wavenumber for the Morse chain. Here $\omega = 2.4$. The solutions were obtained using the finite difference approach.

Minimization with respect to A^2 yields

$$A^2 = \frac{12(\omega^2 - \omega_{\mathrm{h}}^2) - 2W^2/\omega_{\mathrm{h}}^4}{\omega_{\mathrm{h}}^4[\omega_{\mathrm{h}}^4 - 6\omega_{\mathrm{h}}^2 + 18]},$$

which is the same result obtained for FPU in Eq. (9), except for the extra term containing W^2, which is proportional to C_3^2. This means that we will obtain real values for the amplitude A if

$$\omega^2 > \omega_{\mathrm{h}}^2 + \frac{W^2}{6\omega_{\mathrm{h}}^4};$$
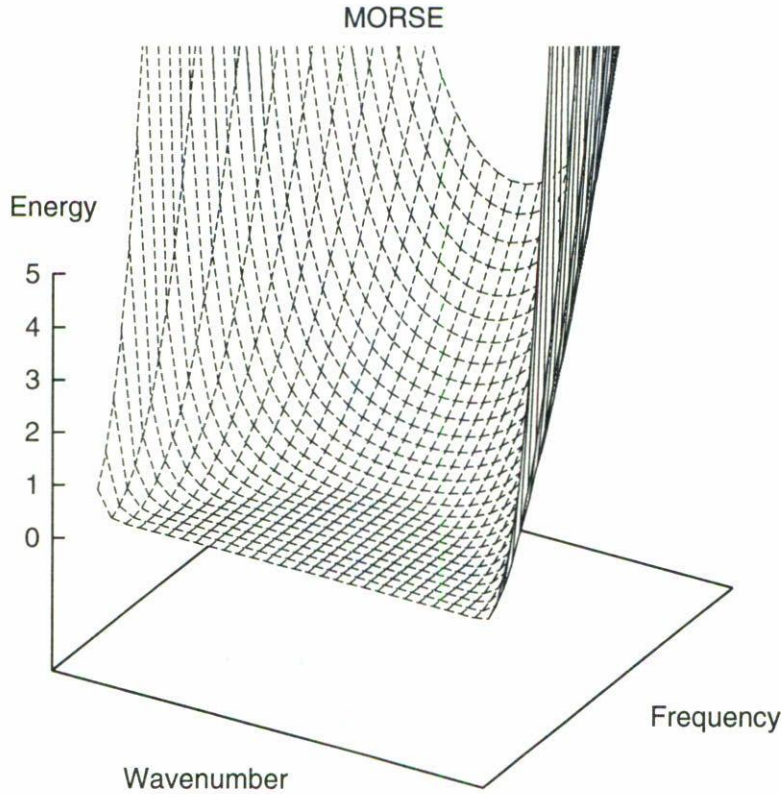
FIGURE 11. Energy surface for the Morse chain, as obtained from the finite differences method. As before, regions of k close to 0 and π are not given since they become numerically out of reach. The wavenumber goes from 0 to 2π and the frequency from 0 to 4.

and therefore, sinusoidal solutions that minimize the error do not start right on the harmonic curve. However, we know that nontrivial solutions do start exactly there, *i.e.*, for $\omega > \omega_{\rm h}$, and we have to conclude that the particular form of the small amplitude limit we have implemented here does not work for potentials with cubic terms. It should be noticed that for the special cases $k = n\pi$, one gets $W = 0$, and so at these values of k the sinusoidal approximations appear at the harmonic curve.

5.2. Continuous limit

The limit of long wavelenght for the LJ potential,

$$V_{\rm LJ} = -\sum_n \frac{1}{36} \left[\frac{1}{2(u_{n+1} - u_n + 1)^{12}} - \frac{1}{(u_{n+1} - u_n + 1)^6} \right],$$

has been investigated by making the same expansion as in Eq. (11), that is, we expand $u_{n\pm 1}$ up to fourth order. Notice that a fully consistent expansion of this potential would also involve a polynomial expansion of the rational expressions. What we do here is only a partial approximation, keeping the rational forms; this allows us to consider cases of large displacements without changing the asymptotic behavior of the potential. It can be
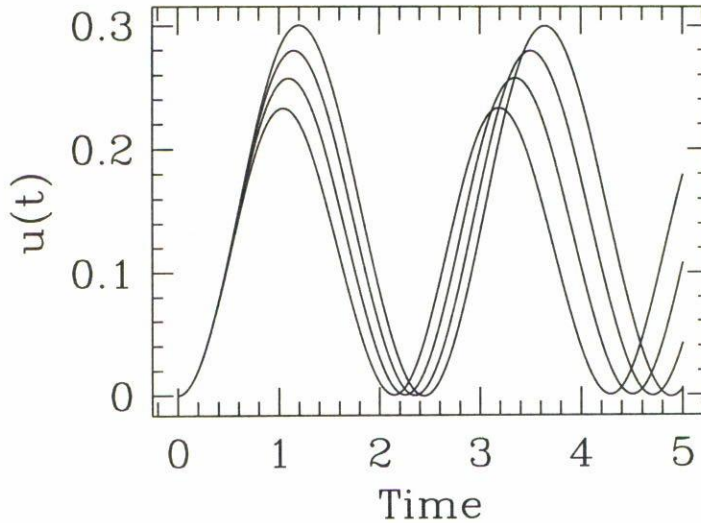
FIGURE 12. Waveforms for 4 different periodic traveling wave solutions for the LJ chain, obtained solving the differential equation (14).

argued that large displacements (u_{n+1} very different from u_n) fail anyway to fulfill the conditions assumed for the long wavelength expansion. This is true, but for intermediate cases it is worthwhile to verify how good this particular approximation can be. Using this expansion the following equation is obtained

$$v^2 u'' + \frac{1}{6}\left[\frac{1}{(f+g)^{13}} - \frac{1}{(f+g)^7} - \frac{1}{(f-g)^{13}} + \frac{1}{(f-g)^7}\right] = 0, \tag{14}$$

where

$$f = u' + \frac{1}{6}u''' + 1, \qquad g = \frac{1}{2}u'' + \frac{1}{24}u'''',$$

come from the Taylor expansion of $u_{n\pm1}$. In order to solve this equation numerically, we need to rewrite it as a system of four first order equations. Defining $u_1 \equiv u'$, $u_2 \equiv u''$, and $u_3 \equiv u'''$, we get for u'''' the following expression:

$$6v^2 u_2 = \left(u_1 + \frac{u_2}{2} + \frac{u_3}{6} + \frac{u''''}{24} + 1\right)^{-13} - \left(u_1 + \frac{u_2}{2} + \frac{u_3}{6} + \frac{u''''}{24} + 1\right)^{-7}$$

$$- \left(u_1 - \frac{u_2}{2} + \frac{u_3}{6} - \frac{u''''}{24} + 1\right)^{-13} + \left(u_1 - \frac{u_2}{2} + \frac{u_3}{6} - \frac{u''''}{24} + 1\right)^{-7}.$$

This equation must be solved self-consistently in each step. This is not a problem since we have verified that it has a unique root for u''''. The system is solved using an adaptive stepsize fourth-order Runge-Kutta method, and the initial conditions used were $u(0) = u'(0) = 0$, $u''(0) \neq 0$, and $u'''(0) \neq 0$. Here $u''(0)$ is used as the independent control parameter, and the value of $u'''(0)$ is adjusted to obtain a solution with zero mean slope, so the solutions are actually periodic.

Several solutions are shown in Fig. 12. As in the case of the FPU system, this are only qualitatively correct, so we think that a different scheme must be used for the investigation in the continuous limit.

6. CONCLUSIONS AND FINAL COMMENTS

We have studied periodic traveling wave solutions for three nonlinear chains: quartic potential (also known as the FPU β-model), Lennard-Jones potential and the Morse potential. The case for the quartic potential was solved numerically, although analytic solutions can be expressed in terms of Jacobi elliptic functions for the small amplitude approximation. Solutions were found only for values of k and ω such that $\omega(k) \geq \omega_\mathrm{h}(k)$, *i.e.*, above the harmonic dispersion curve. This is a similar situation with a spring subjected to a "hard" return force: the frequency is shifted upwards [5]. Although this is well known for a single oscillator, it is not an obvious result for a chain. The solutions are small-amplitude, almost sinusoidal functions when ω is close to ω_h, but tend to a rectangular step as we raise ω above from the harmonic value or approach $k = 0$ or $k = 2\pi$ (Figs. 1 and 2). The energy per particle was found [see Eq. (6)] as a function of ω and k, confirming that there are no solutions below the harmonic dispersion curve.

As a test of the usual sinusoidal solution for the small amplitude limit, we introduced an approximate solution $u(t) = A\sin(\omega t)$, and varied A to minimize the error with respect to the actual differential equation. From this approach we get an analytic confirmation that real values for the amplitude A exist only if $\omega^2 \geq \omega_\mathrm{h}^2$, as it was seen from the numerical results.

In the continuous limit (for wavelenghts much greater than the lattice constant), we used an approximate solution by taking the four leading terms in the Taylor expansion of the solutions $u_{n\pm1}(t)$, and got a differential equation which was numerically solved assuming traveling wave solutions. The solutions obtained are correct only qualitatively.

The Morse and Lennard-Jones Potentials were solved in an analogous way as we did for the FPU case. We found the same kind of behavior except that the limiting solutions are of the form of a saw-tooth wave. The small amplitude limit did not gave correct results when applied to these systems. We show how the presence of the cubic term in the potential is responsible for this failure and a different approach must be implemented.

Finally, the continuous limit for the Lennard-Jones potential was investigated giving as before only qualitative results, so a careful examination of the approximations made is necessary in a future work in order to get better results in this limit.

REFERENCES

1. N.W. Ashcroft and N.D. Mermin, *Solid State Physics*, Holt, Reinhart, and Winston, Philadeiphia (1976), Chap. 30.
2. G.P. Srivastava, *The Physics of Phonons*, Adam Hilger, Bristol, (1990).
3. R. Rajaraman, *Solitons and Instantons*, North-Holland, Amsterdam, (1982).

4. N.J. Zabusky and M.D. Kruskal, *Phys. Rev. Lett.* **15** (1965) 240.
5. I.G. Main, *Vibrations and Waves in Physics*, Cambridge University Press, Cambridge, (1993).
6. E. Desurvire, *Physics Today,* **47** (1994) 20.
7. D.J. Korteweg and G. de Vries, *Phyl. Mag.* **39** (1895) 422.
8. P.G. Drazin and R.S. Jonhson, *Solitons: an introduction*, Cambridge University Press, (1989).
9. P.G.Drazin, *Quart. J. Mech. Appl. Math.* **30** (1977) 91.
10. C.F. Driscol and T.M.O'Neil, *Phys. Rev. Lett.* **37** (1976) 69.
11. M. Toda, *J. Phys. Soc. Jpn.* **22** (1967) 431; see also M. Toda, *Theory of nonlinear lattices*, Solid State Science, Vol. 20, Springer, Berlin (1981).
12. Y.S. Kirchar, *Phys. Rev. E***48** (1993) R43.
13. R. Dusi and M. Wagner, *Phys. Rev. B***51** (1995) 15847.
14. A.J. Sievers and S.Takeno, *Phys.Rev.Lett.* **61** (1988) 970.
15. K.W. Sandusky and J.B. Page, *Phys. Rev. B***50** (1994) 866.
16. T. Rösseler and J.B. Page, *Phys. Lett. A***204** (1995) 418.
17. P. Poggi and S. Ruffo, preprint chao-dyn/9510017 at Los Alamos e-print repository xyz (http://xyz.lanl.gov) (1995).
18. J. Ford, *Phys. Rep.* **213** (1992) 271.
19. E. Fermi, J. Pasta and S. Ulam, Los Alamos Scientific report, (1955) (unpublished). Also in *The collected papers of Enrico Fermi*, Vol. 2, pp. 977-989, University of Chicago Press, Chicago (1965).
20. W.H. Press *et al.*, *Numerical Recipes in Fortran: The Art of Scientific Computing*, Cambridge University Press, New York (1992).
21. Goldstein, *Classical Mechanics*, Addison Wesley, New York, (1980).
22. A.J. Lichtenberg and M.A. Lieberman, *Regular and Chaotic Dynamics*, Springer-Verlag, New York, (1992).
23. M. Abramowitz and I. Stegun, *Handbook of Mathematical Functions*, Dover, New York (1972).
24. W.W. Wood and F.R. Parker, *J. Chem. Phys.* **27** (1957) 720.
25. L. Verlet, *Phys. Rev.* **159** (1967) 98.